

Postdoc Fellowships for non-EU researchers

Final Report

Name	Priyanka Shukla
Selection	2013
Host institution	ULB, Brussels
Supervisor	Prof. Anne De Wit
Period covered by this report	From 20/3/2014 to 19/07/2015
Title	Chemically-driven fingering instabilities

1 Objectives of the Fellowship

Our objectives are to study dynamics of chemically driven fingering instabilities in a porous medium numerically. Particularly, we are interested in analyzing the properties of viscous and precipitation fingering driven by a simple $A + B \rightarrow C$ type chemical reaction, and to compare them with those of non-reactive fingering patterns. In order to achieve set goals of the fellowship, we employ reaction-diffusion-convection (RDC) model consists of RDC equations for concentrations of the reactants and the product coupled with the equations for balance of mass and momentum.

Our research work is based on the observations from the experiments [14, 16, 18], theory [9, 22] and simulations [7, 13, 22], which show that the reaction can destabilize the classically stable situation of a less mobile (e.g. more viscous) fluid displacing a more mobile (e.g. less viscous) one. It has been found that reactive viscous fingering occurs if the product has a viscosity either larger or smaller than the viscosity of the reactants. Similarly, the precipitation fingering driven by a precipitation reaction occurs if the product decreases the permeability of the porous medium. In the reverse case, when the product increases the permeability, the resulting fingering is known as dissolution fingering. A RDC model of similar problems [7, 13] is adapted to account gradients in viscosity and permeability. Such reaction induced gradients in viscosity and permeability are responsible for reactive fingering instability. In this context two types of problems can be classified:

Precipitation fingering

Nagatsu et al. [14] have recently shown that a localized precipitation reaction, induced by a simple $A + B \rightarrow C$ type reaction when a solution of A invades a solution of B with C being the solid product, can trigger fingering in the zone where the more mobile solution of A displaces the less mobile precipitate C . This precipitation-driven fingering is of interest due to its applications in CO_2 sequestration and mineralization [25, 26]. In the case of precipitation, the solid product can barely diffuse, which is quite different from reactive viscous fingering (VF) in which the reactants A , B and the product C can have diffusion coefficients of the same order of magnitude. The important question is whether this slow diffusivity of the precipitation product C impacts the physical and statistical properties of precipitation patterns. *In this context, the objective of the present study is to investigate numerically the characteristics of precipitation-driven fingering patterns numerically and to compare them with those of reactive VF patterns [7], and in particular to investigate the influence of the fact that the precipitate does not diffuse much.*

Viscous fingering

The experimental study of Nagatsu et al. [16] showed that at large injection rate, or Pe number (ratio of the convective to diffusion transport rates), an instantaneous chemical reaction changes

the viscosity of the solutions, and thereby leading to miscible VF when a less-viscous acidic (or basic) solution, solution A , is injected radially into a more viscous polymeric solution, solution B , in a Hele-Shaw cell. Depending on the reaction-induced increase or decrease of viscosity of the displacing solution (solution B), two types of observations were made. In the former case VF pattern was observed to be denser than that of non-reactive case whereas less-denser VF pattern was reported in the latter case (viscosity decrease).

Recently, Nagatsu et al. [15] carried out new experiments focusing on the influence of injection rate on viscosity increasing and decreasing systems. Interestingly, the opposite effects of the reaction on the VF pattern have been observed at large and small Pe for both systems showing viscosity increase and decrease by the reaction. When the reaction increases the viscosity of the displacing solution, a less dense VF pattern is observed for low Pe and a denser one at high Pe. In contrast, opposite effects are observed in the system where the reaction decreases the viscosity of the displacing solution i.e. denser VF patterns at small Pe and less dense one at high Pe. Later the same experiments have been carried out for wider range of Pe number in order to confirm the validity of this opposite behavior of VF pattern as a function Pe. The opposite behavior as a function of Pe is confirmed for the case of viscosity decreasing system, whereas the viscosity increasing system ceases to show this behavior. In brief, experiments shows that in the viscosity decreasing systems, the reactive VF can be controlled by the Pe number or injection rate. Moreover when the viscosity decrease by the reaction is large enough, a stabilisation of the reactive VF instability is obtained at small Pe. *In this problem, our objectives are to study this experimentally-observed stabilisation mechanism of reactive VF at low Pe number. Specifically, we do the mathematical modelling of above experiment using RDC equations and solve numerically.*

2 Methodology in a nutshell

To analyse theoretically chemically-driven viscous and precipitation fingering, we followed following methodology.

- Developed theoretical reaction-diffusion-convection (RDC) models consist of RDC equations for concentrations of the reactants and the product coupled with the equations for balance of mass and momentum (Darcy’s law).
- Developed pseudospectral based numerical codes for integrating the RDC models for both the problems namely precipitation and reactive viscous fingering.
- Carried out parametric analysis. Mainly the effect of Peclet number (Pe) in reactive VF, and effect of diffusivity of the product in precipitation fingering problems.
- Compared simulations with experimental results obtained by Nagatsu et al. for reactive VF [15, 16], and precipitation fingering [14].

3 Results

In the following we show the outcomes of our research on precipitation fingering and reactive viscous fingering.

3.1 Precipitation fingering

As described above, the objective of this study is to investigate numerically the characteristics of precipitation-driven fingering patterns numerically. In order to do so, the RDC model of precipitation driven fingering [14] is modified to allow the diffusivity of the solid product to tend

to zero. We show that this slow diffusivity of the precipitate has important consequences on the fingering patterns including much earlier destabilization and smaller wavelength.

The Model: We consider a homogeneous two dimensional porous medium or a horizontal thin Hele-Shaw cell, of length L_x and width L_y with initial permeability κ_0 . In this system, a solution of reactant B in initial concentration b_0 is sandwiched between solutions of reactant A with concentration a_0 ($a_0 \leq b_0$). We assume that the viscosity μ and density ρ of the two solutions are equal and constant. Such an initial configuration allows to study two cases—namely, when A invades B and vice-versa—simultaneously in one single numerical simulation. The initial positions of the left and right miscible interfaces, where A and B come into contact and react, are x_l and x_r , respectively. The solutions are displaced from left to right at a constant speed U such that the solution A displaces the solution B at $x = x_l$ while the solution A is being displaced by the solution B at $x = x_r$. A precipitation reaction of type $A + B \rightarrow C$ takes place at the miscible interfaces producing a solid product C in the reactive zone around the initial contact lines. This solid precipitate is present in the solution as small particles that can diffuse in the solvent with a low diffusivity D_C and be advected by the flow. Its concentration in the solvent is denoted by c . We assume that the presence of the precipitate C does not change the density ρ and the viscosity μ of the solvent, which are thus kept constant. Moreover, we assume that the porosity ϕ remains roughly constant and that the solid phase changes only substantially the permeability κ of the porous matrix.

We analyse here the fingering instability which arises due to changes in the permeability κ of the porous medium by a precipitation reaction for a constant viscosity μ , density ρ and porosity ϕ . Fingering develops locally in the zone where the reactant solution with reference permeability κ_0 (or mobility $M_0 = \kappa_0/\mu$) pushes the solution of the precipitate C of lower permeability (or lower mobility). The flow field, considered as incompressible (1), follows Darcy's law (2) coupled to the evolution equations for the concentrations (3)–(5) via the permeability $\kappa = \kappa(c)$ (6) which is a function of the local concentration $c(x, y, t)$ of the product C . The resulting RDC model reads [3, 4, 7–9, 13, 14]:

$$\nabla \cdot \mathbf{u} = 0, \quad (1)$$

$$\nabla p = -\frac{\mu}{\kappa(c)}\mathbf{u}, \quad (2)$$

$$\frac{\partial a}{\partial t} + \mathbf{u} \cdot \nabla a = D_A \nabla^2 a - k a b, \quad (3)$$

$$\frac{\partial b}{\partial t} + \mathbf{u} \cdot \nabla b = D_B \nabla^2 b - k a b, \quad (4)$$

$$\frac{\partial c}{\partial t} + \mathbf{u} \cdot \nabla c = D_C \nabla^2 c + k a b, \quad (5)$$

where (a, D_A) , (b, D_B) , and (c, D_C) denote the (concentration, diffusion coefficient) of species A , B and C , respectively, p is the pressure, $\mathbf{u} = (u, v)$ is the two-dimensional velocity vector, and k is the kinetic constant. By analogy with previous works on classical VF [17, 21–24, 27] or studies of rock dissolution [2, 10, 20] and reactive VF [7–9, 13], the permeability of the system is assumed to be a decreasing function of the product concentration as [14]

$$\kappa(c) = \kappa_0 e^{-R(c/a_0)}, \quad (6)$$

where κ_0 is the permeability when $c = 0$ i.e. in absence of any precipitate. Let $\kappa_m = \kappa(a_0) = \kappa_0 e^{-R}$ be the permeability when $c = a_0$. The parameter $R = \ln(M_0/M_m)$ is then defined as the log-mobility ratio where $M_0 = \kappa_0/\mu$ and $M_m = \kappa_m/\mu$ are the mobilities when $c = 0$ and $c = a_0$, respectively. The parameter R quantifies the influence of precipitation on permeability changes. When $R > 0$, the precipitate C reduces the permeability of the porous matrix locally.

In the precipitation case, the product C barely moves i.e. D_C is small. To take this specificity into account, we use here the diffusivity D_A of the reactant A as a reference scale for diffusivity.

The reference scales for velocity, time, length, concentration, permeability, and pressure are thus taken as U , D_A/U^2 , D_A/U , a_0 , κ_0 , and $\mu D_A/\kappa_0$, respectively. For simplicity, we write equations (1)–(6) in a reference frame moving with velocity U i.e. the flow direction x and flow velocity \mathbf{u} are transformed as $x' = x - Ut$ and $\mathbf{u}' = \mathbf{u} - U\mathbf{e}_x$, respectively, with \mathbf{e}_x being the unit vector along the x direction. The dimensionless form of (1)–(6) in the moving frame becomes

$$\nabla \cdot \mathbf{u} = 0, \quad (7)$$

$$\nabla p = -\frac{1}{\kappa(c)}(\mathbf{u} + \mathbf{e}_x), \quad (8)$$

$$\frac{\partial a}{\partial t} + \mathbf{u} \cdot \nabla a = \nabla^2 a - D_a a b, \quad (9)$$

$$\frac{\partial b}{\partial t} + \mathbf{u} \cdot \nabla b = \delta_b \nabla^2 b - D_a a b, \quad (10)$$

$$\frac{\partial c}{\partial t} + \mathbf{u} \cdot \nabla c = \delta_c \nabla^2 c + D_a a b, \quad (11)$$

$$\kappa(c) = e^{-R c}, \quad (12)$$

where $D_a = D_A k a_0 / U^2$ is the dimensionless Damköhler number which quantifies the ratio of the hydrodynamic time scale $\tau_h = D_A / U^2$ to the chemical time scale $\tau_c = 1 / k a_0$, and $\delta_b = D_B / D_A$ and $\delta_c = D_C / D_A$ are the diffusion coefficient ratios. Taking the curl of the momentum equation (8) and introducing the stream function ψ as $u = \partial\psi/\partial y$ and $v = -\partial\psi/\partial x$, we get

$$\nabla^2 \psi = R(\psi_x c_x + \psi_y c_y + c_y), \quad (13)$$

$$a_t + a_x \psi_y - a_y \psi_x = \nabla^2 a - D_a a b, \quad (14)$$

$$b_t + b_x \psi_y - b_y \psi_x = \delta_b \nabla^2 b - D_a a b, \quad (15)$$

$$c_t + c_x \psi_y - c_y \psi_x = \delta_c \nabla^2 c + D_a a b. \quad (16)$$

The initial conditions for the stream function and product concentration are $\psi(x, y) = 0$ and $c(x, y) = 0$, for all (x, y) , respectively. For the initial condition of the concentrations, we use two back to back step functions centered at the two locations x_l and x_r between A and B with a random noise being introduced at x_l and x_r [7]:

$$[a(x, y), b(x, y)] = \begin{cases} [1, 0] & \text{for } 0 \leq x < x_l, \\ [\frac{1}{2}(1 + \zeta r), \frac{1}{2}(1 - \zeta r)\phi] & \text{for } x = x_l \\ [0, \phi] & \text{for } x_l < x < x_r \\ [\frac{1}{2}(1 - \zeta r), \frac{1}{2}(1 + \zeta r)\phi] & \text{for } x = x_r \\ [0, 1] & \text{for } x_r < x < \text{Pe}' \end{cases} \quad (17)$$

for all $0 \leq y < \text{Pe}$, where $\phi = b_0/a_0$ is the initial concentration ratio of solutions A and B , r is a random number between 0 and 1, and ζ is an amplitude of order 10^{-2} . The Péclet numbers $\text{Pe}' = UL_x/D_A$ and $\text{Pe} = UL_y/D_A$ represent the dimensionless length and width of the numerical domain. The dynamics of reactive precipitation fingering depends on five parameters, namely, R , D_a , δ_b , δ_c and ϕ . To integrate equations (13)–(16) numerically, we use a pseudospectral numerical scheme [1, 3–5, 7, 22] with periodic boundary conditions along both directions. The physical domain $\text{Pe}' \times \text{Pe}$ is taken to be 256×64 . In order to handle sharp jumps in the initial conditions leading to Gibb's phenomenon [22], we use a small spatial step $dx = dy = 0.125$ (i.e. 2048×512 spectral modes) and time step $dt = 0.0025$.

Outcomes: In the symmetric case, for which the reactants A and B have the same initial concentration ($\phi = 1$) and diffusion coefficients ($\delta_b = 1$), the concentrations of the product C is shown in figure 1 for $\delta_c = 0.01$, $R = 2$, and $D_a = 1$. It is seen that, as time evolves, A and B meet, react, and are transformed through the reaction to a solid precipitate C in the reactive zone. This solid precipitate changes locally the permeability of the porous medium,

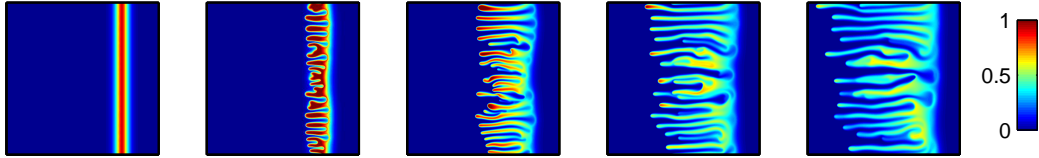


Figure 1: Concentration of the product C for $\delta_c = 0.01$, $\delta_b = 1$, $\phi = 1$, $R = 2$, and $D_a = 1$, at $t = 20$, 40, 60, 80, and 100 (from left to right).

and, hence, the mobility of the solution. Consequently, a situation arises where locally a high mobility solution of A invades a low mobility zone containing C which triggers the fingering instability, as shown in figure 1.

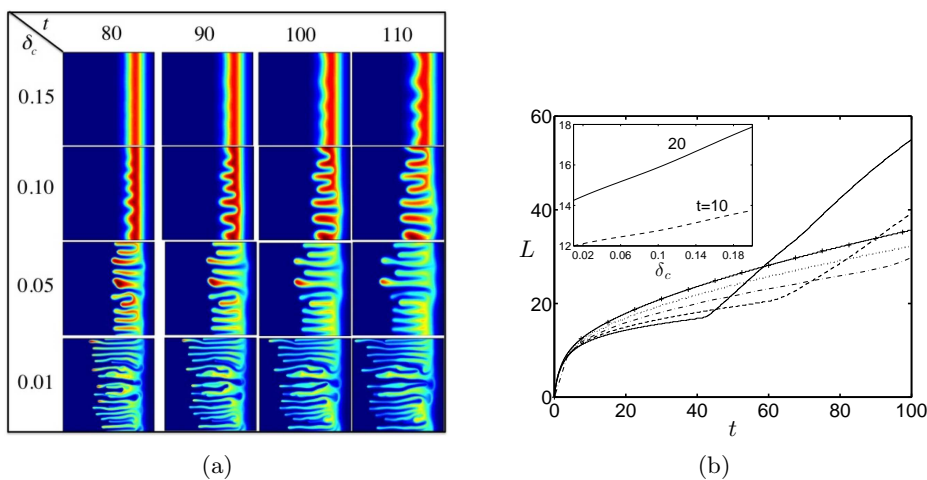


Figure 2: (a) Comparison of the concentrations of the product for decreasing values of δ_c at $t = 80$, 90, 100, and 110. (b) Temporal variation of the mixing length L for various values of $\delta_c = 0.01$ (solid line), 0.05 (dashed line), 0.1 (dash-dotted), 0.15 (dotted), 0.2 (solid line with plus symbol). The inset shows the variation of L with δ_c for two values of $t = 10$ and 20. The other parameters are the same as in figure 1.

To see the effect of varying δ_c on the nonlinear fingering pattern, the concentrations of the product are shown in figure 2(a) for $\delta_c = 0.1, 0.1, 0.05$ and 0.01 . The instability starts earlier and the number of fingers increases with decreasing δ_c , i.e. the system becomes more unstable as $\delta_c \rightarrow 0$. This is related to the fact that the unfavorable gradient $d\kappa/dx$ becomes steeper when $\delta_c \rightarrow 0$. We can next compute the mixing length L of the product C defined as the length of the zone where a precipitate is present. Figure 2(b) shows the variation of this mixing length with time for various values of δ_c . In the diffusive regime, the mixing length follows a square root scaling with time i.e. $L \propto \alpha\sqrt{t}$ where α depends on the diffusivity of the reactants and product [6]. The inset shows that in the diffusive regime the mixing length depends on δ_c . In the transition regime, the mixing length deviates from the diffusive \sqrt{t} scaling once the system enters into the convective regime for which the mixing length varies linearly with time.

Conclusions: We have numerically studied the properties of precipitation-driven fingering when a solution of a reactant A displaces a solution of B to produce a solid product C in the miscible reactive zone. It has been found that decreasing D_C destabilizes the system and that, in this limit of $D_C \rightarrow 0$, the onset time of precipitation fingering is much faster than that of reactive VF. This is the case when the ratio of the initial concentrations and the diffusivity ratio of the reactants are equal to one ($\phi = 1, \delta_b = 1$). Failing any of these conditions, when

$\phi \neq 1$ or $\delta_b \neq 1$ (we refer [19] for more detail), lead to asymmetric RD concentration profiles, subsequently leading to different precipitation patterns whether A displaces B or the reverse. Our results show that the system is more unstable with regard to precipitation fingering when the invading solution is either more concentrated or contains the fastest diffusing reactant.

3.2 Reactive viscous fingering

In this problem, we investigate numerically the influence of changes in the injection flow rate or equivalently the Péclet number, Pe , on the reactive viscous fingering instability. We analyse fingering patterns for different values of Pe at moderate Damköhler number, D_a . By analyzing fingering patterns for viscosity-decreasing reactive systems at low and high Péclet numbers, we show that the reaction shows stabilising and destabilising effects, respectively, with regard to non-reactive systems.

The Model: Let us consider a homogeneous two-dimensional porous medium or Hele-shaw cell of length L_x and width L_y with constant permeability $\kappa = l^2/12$ where l ($l \ll L_x, L_y$) is the gap between the plates. A miscible solution of reactant A in initial concentration a_0 with viscosity μ_A is injected into a solution of reactant B in initial concentration b_0 with viscosity μ_B . We assume that the initial concentrations and density of the two solutions are equal, further the density is assumed to be constant. The initial position of the miscible interface, where the two solutions come across and react, is x_0 . The solution B is displaced from left to right with a constant speed U along the x -direction. A simple chemical reaction of type $A + B \rightarrow C$ takes place, at the miscible interface between A and B , and gives the product C of viscosity μ_C in the reactive zone around interface. Similar to the precipitation problem, we assume incompressible and neutrally buoyant system satisfying following equations:

$$\nabla \cdot \mathbf{u} = 0, \quad (18)$$

$$\nabla p = -\frac{\mu(a, b, c)}{\kappa} \mathbf{u}, \quad (19)$$

$$\frac{\partial a}{\partial t} + \mathbf{u} \cdot \nabla a = D_A \nabla^2 a - k a b, \quad (20)$$

$$\frac{\partial b}{\partial t} + \mathbf{u} \cdot \nabla b = D_B \nabla^2 b - k a b, \quad (21)$$

$$\frac{\partial c}{\partial t} + \mathbf{u} \cdot \nabla c = D_C \nabla^2 c + k a b, \quad (22)$$

where the symbols are the same as in equations (1)–(5). The viscosity of the solutions of reactants A and B and product C is defined as μ_A , μ_B and μ_C , respectively, when only one species present in concentration a_0 . We assume the viscosity as an exponential function of the concentrations of A , B and C as

$$\mu(a, b, c) = \mu_A e^{R_b(b/a_0) + R_c(c/a_0)}, \quad (23)$$

where R_b and R_c are the log-mobility ratios and are defined as

$$R_b = \ln \left(\frac{\mu_B}{\mu_A} \right) \quad \text{and} \quad R_c = \ln \left(\frac{\mu_C}{\mu_A} \right). \quad (24)$$

For the non-reactive case or the case when the product C has the same viscosity as one of the reactant ($R_b = R_c$), the system is genuinely believed to be unstable (stable) if the lower (higher) viscosity solution displaces the higher (lower) viscosity solution i.e. $\mu_A < \mu_B$ or $R_b > 0$ ($\mu_A > \mu_B$ or $R_b < 0$).

For non-dimensionalization, the reference scales for velocity, length, time, concentration, viscosity, diffusivity, and pressure are taken as U , L_y , L_y/U , a_0 , μ_A , D_C , and $\mu_A U L_y / \kappa$, respectively, and for simplicity, equations are expressed in a frame moving with speed U by using

transformation $x \rightarrow x - Ut$ and $\mathbf{u} \rightarrow \mathbf{u} - U\mathbf{e}_x$ with \mathbf{e}_x being the unit vector along the x direction. If we take the curl of the momentum equation and define the stream function $\psi(x, y)$ as $u = \partial\psi/\partial y$ and $v = -\partial\psi/\partial x$, we get

$$\nabla^2\psi = R_b(\psi_x b_x + \psi_y b_y + b_y) + R_c(\psi_x c_x + \psi_y c_y + c_y), \quad (25)$$

$$a_t + a_x\psi_y - a_y\psi_x = \frac{\delta_a}{Pe}\nabla^2 a - D_a a b, \quad (26)$$

$$b_t + b_x\psi_y - b_y\psi_x = \frac{\delta_b}{Pe}\nabla^2 b - D_a a b, \quad (27)$$

$$c_t + c_x\psi_y - c_y\psi_x = \frac{1}{Pe}\nabla^2 c + D_a a b, \quad (28)$$

$$\mu(a, b, c) = e^{R_b b + R_c c}, \quad (29)$$

where $D_a = L_y k a_0 / U$ is the dimensionless Damköhler number and, $\delta_a = D_A / D_C$ and $\delta_b = D_B / D_C$ are the diffusion coefficient ratios. The reaction rate \mathcal{R} is defined as $D_a a b$. The initial conditions are chosen as $\psi(x, y) = 0$ and $c(x, y) = 0$, for all (x, y) , and step functions between solutions A and B are used for the initial concentrations of A and B . The above set of equations (25)–(29) are solved using pseudospectral numerical method. The computations are performed using discrete Fourier transform library FFTW 3.3.4.

Outcomes: Figure 3 shows the concentrations, viscosity, and reaction rate for $D_a = 1$, $R_b = 2$ and $R_c = -2$ with two values of Péclet numbers: $Pe = 100$ and 1000 . We see that at $Pe = 100$, fingering between A and C decays in time as soon as the viscosity decreases in this zone. On the other hand, fingering remains in the zone between the product C and the solution B . Nevertheless, the fingering between C and B is stabilising eventually because of transverse diffusion. It is seen that the viscosity quickly develops a minimum at the reactive zone and the reaction rate is not advected along the transverse direction, see figure 3(d–e).

The second column of figure 3(f–j) show the reactive fingering at $Pe = 1000$. We know that the non-reactive system is more unstable for large Pe [11], which remains true for reactive system as well. As seen from figure 3(f–j) that the fingering starts earlier than the small Pe . The coarsening, shielding and tip splitting are encountered more often for large Pe as compared to the case of non-reactive and low Pe . The above observations have been reported by Nagatsu and De Wit [13]. We see from the viscosity fields, see figure 3(d,i), that the viscosity minimum (shown by dark blue) is not fully developed rather it covers a thin region around the fingers. Furthermore, we notice that the reaction rate is larger at the tip which makes fingers to elongate more in A -rich region.

The mixing lengths—length of the zone where the mixing occurs—of the solutions of A and B for two reactive VF cases at $D_a = 1$ and $D_a = 4$ (solid and dashed lines), and non-reactive (dot-dashed line) VF case are shown in figure 4. For small Pe , the instability starts earlier, and the onset time decreases with increasing D_a . Therefore, the reactive VF is always more unstable than that of the non-reactive VF at early time. As seen from figure 4(a) that, in contrast to the non-reactive case (red solid line), the mixing length of A for reactive case (green and blue solid lines) first increases rapidly until a maximum value and then decreases. For large Pe , see figure 4(b), the mixing length of A and B both increases in time for the reactive and the non-reactive cases. It is seen that the mixing length of the reactive VF is always more than that of the non-reactive case, which implies that at high Pe the reactive VF is more unstable than that of the non-reactive one.

Conclusion: We numerically analysed the problem of reactive VF for various flow rates, or in terms of control parameter, Péclet number (Pe). We showed that at low Péclet number, the chemical reaction shows stabilising effect for a chemical species (A or B). In other words, depending on the flow rate (Pe), the chemical reaction may enhance or suppress fingering instability. This stabilisation at low Péclet number has been shown to be related to the viscosity minimum which is developed around the interface due to chemical reaction. The present results agree qualitative with the experiments of Nagatsu et al. [15, 16].

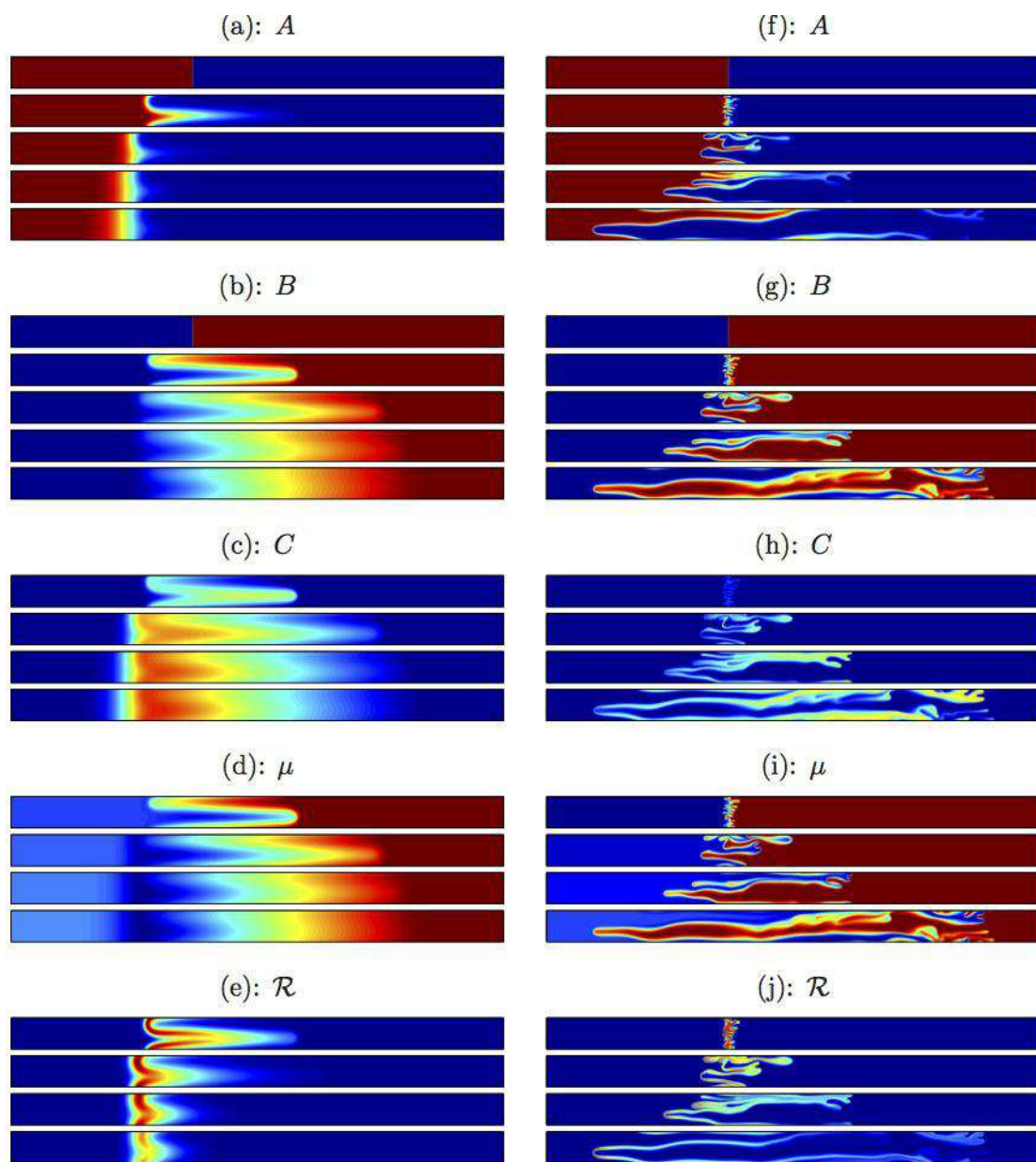


Figure 3: Reactive fingering at $R_b = 2$, $R_c = -2$ and $Da = 1$. The first figure in (a,h) and (b,i) represents the initial concentrations of A and B respectively. Concentration fields A , B , C , μ and \mathcal{R} for (a–e) $Pe = 100$ at $t = 10, 20, 30, 40$ and (f–j) $Pe = 1000$ at $t = 1, 3, 5, 10$. Other parameters are $R_c = -2$, $R_b = 2$ and $Da = 1$. In color-scale A and B are scaled between zero and one, C is scaled between zero and half, and μ and the reaction $\mathcal{R} = D_a ab$ are shown in their absolute values.

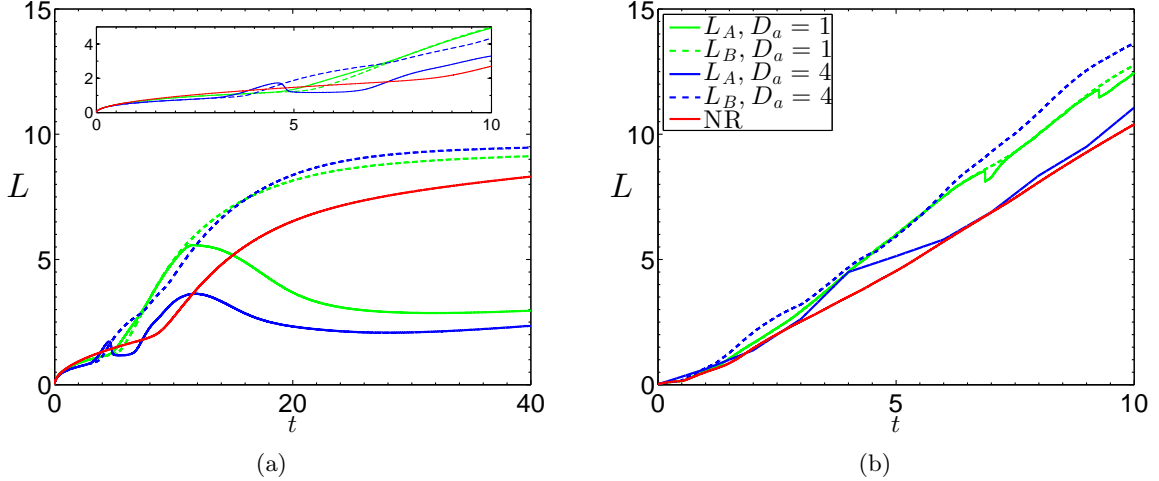


Figure 4: Temporal evolution of mixing lengths of A and B for (a) $Pe = 100$, and (b) $Pe = 1000$. For $D_a \neq 0$, solid and dashed lines denote the mixing length of A and B , respectively. Green: $D_a = 1$, Blue: $D_a = 4$, Red: $D_a = 0$ (non-reactive).

4 Perspectives for future collaboration between units

First problem ‘on the precipitation fingering’ has already been published in an international journal [19]. Second problem, which deals with the reactive viscous fingering, is ongoing. We shall submit our manuscript to an international journal, shortly. In future, we would like to study nonlinear dynamics of fingering patterns arising due to an interplay between viscous and precipitation driven fingering. We are also interested in linear stability analysis of these problems. There is a lot of scope for collaboration as both units, host (NLPC at ULB) and home (Dept. of Mathematics, IITM) departments, have interdisciplinary vision [12]. The beneficiary (Dr. Shukla) has recently formed a research group inclined on fluid mechanics problems. During postdoctoral stay, the beneficiary has gained simulation skills which certainly will be helpful in validating experimental results on Hele-Shaw cell carried out at ULB (De Wit’s lab) and other institutions. One such collaborative research already appeared in Physical Review E [19]. This gives a positive signal for future collaboration between units.

5 Valorisation/Diffusion (including Publications, Conferences, Seminars, Missions abroad...)

1. Fingering dynamics driven by a precipitation reaction: Nonlinear simulations, Shukla P. & De Wit A., Phys. Rev. E, **93**, pp. 023103, 2016 [19].
2. Fingering instability driven by a simple precipitation reaction, Shukla P. & Wit De A., IUTAM Symposium on Multiphase flows with phase change challenges and opportunities, Hyderabad, India. Dec. 8–11, 2014.

6 Skills/Added value transferred to home institution abroad

Added value transferred to home institution is to develop contact with European research and European collaborator of De Wit’s group within the ESA Topical Team in which the project is performed. Skills transferred to beneficiary, as well as home institution, are to carry out nonlinear simulations of chemo-hydrodynamic systems. Moreover, the skills developed during postdoctoral stay enabled the beneficiary to start own independent research group on fluid

mechanics, mostly dealing with hydrodynamic instabilities, at home institution (IITM). Clearly, this independent research group is added value to the home institution (IITM). Furthermore, the beneficiary has gained knowledge that there are already existing independent research groups (for instance Prof. S. Pushpavanam, Chemical Engineering Department at IIT Madras) working on chemo-hydrodynamic systems (research theme of the fellowship). Thus, the beneficiary’s research group, which is also focused on chemo-hydrodynamic systems, will strengthen (value-added) research on chemo-hydrodynamics at home institute.

References

- [1] C. Canuto, M. Y. Hussani, A. Quarteroni, and T. A. Zang. *Spectral Methods in Fluid Dynamics*. Springer, 1988.
- [2] J. Chadam, D. Hoff, E. Merino, P. Ortoleva, and A. Sen. Reactive infiltration instabilities. *IMA J. Appl. Math.*, 36:207–221, 1986.
- [3] A De Wit and G. M. Homsy. Nonlinear interactions of chemical reactions and viscous fingering in porous media. *Phys. Fluids*, 11:949, 1999.
- [4] A De Wit and G. M. Homsy. Viscous fingering in reaction-diffusion systems. *J. Chem. Phys.*, 110:8663, 1999.
- [5] B. Fornberg. *A Practical Guide to Pseudospectral Methods*. Cambridge Monographs on Applied and Computational Mathematics. Cambridge University Press, 1998.
- [6] L. Gálfi and Z. Rácz. Properties of the reaction front in an $A + B \rightarrow C$ type reaction-diffusion process. *Phys. Rev. A*, 38:3151–3154, 1988.
- [7] T. Gérard and A. De Wit. Miscible viscous fingering induced by a simple $A + B \rightarrow C$ chemical reaction. *Phys. Rev. E*, 79:016308, 2009.
- [8] S. H. Hejazi and J. Azaiez. Hydrodynamic instability in the transport of miscible reactive slices through porous media. *Phys. Rev. E*, 81:056321, 2010.
- [9] S. H. Hejazi, P. M. J. Trevelyan, J. Azaiez, and A. De Wit. Viscous fingering of a miscible reactive $A + B \rightarrow C$ interface: a linear stability analysis. *J. Fluid Mech.*, 652:501–528, 2010.
- [10] E. J. Hinch and B. S. Bhatt. Stability of an acid front moving through porous rock. *J. Fluid Mech.*, 212:279–288, 3 1990.
- [11] G M Homsy. Viscous fingering in porous media. *Annu. Rev. of Fluid Mech.*, 19(1):271–311, 1987.
- [12] IIT Madras. Strategic plan 2020, January 2014.
- [13] Y. Nagatsu and A De Wit. Viscous fingering of a miscible reactive $A + B \rightarrow C$ interface for an infinitely fast chemical reaction: Nonlinear simulations. *Phys. Fluids*, 23:043103, 2011.
- [14] Y. Nagatsu, Y. Ishii, Y. Tada, and A De Wit. Hydrodynamic fingering instability induced by a precipitation reaction. *Phys. Rev. Lett.*, 113:024502, 2014.
- [15] Y. Nagatsu, T. Masumo, and A. De Wit. Effect of the injection rate on changes in the density of viscous fingering patterns affected by an instantaneous chemical reaction. *Report*, xxx:1–15, 2015.

- [16] Y. Nagatsu, K. Matsuda, Y. Kato, and Y. Tada. Experimental study on miscible viscous fingering involving viscosity changes induced by variations in chemical species concentrations due to chemical reactions. *J. Fluid Mech.*, 571:475–493, 2007.
- [17] S. Pramanik and M. Mishra. Effect of pećlet number on miscible rectilinear displacement in a hele-shaw cell. *Phys. Rev. E*, 91:033006, 2015.
- [18] L. A. Riolfo, Y. Nagatsu, S. Iwata, R. Maes, P. M. J. Trevelyan, and A. De Wit. Experimental evidence of reaction-driven miscible viscous fingering. *Phys. Rev. E*, 85:015304, 2012.
- [19] P. Shukla and A. De Wit. Fingering dynamics driven by a precipitation reaction: Nonlinear simulations. *Phys. Rev. E*, 93:023103, 2016.
- [20] P. Szymczak and Anthony J. C. Ladd. Reactive-infiltration instabilities in rocks. part 2. dissolution of a porous matrix. *J. Fluid Mech.*, 738:591–630, 2014.
- [21] C. T. Tan and G. M. Homsy. Stability of miscible displacements in porous media: Rectilinear flow. *Phys. Fluids*, 29:3549, 1986.
- [22] C. T. Tan and G. M. Homsy. Simulation of nonlinear viscous fingering in miscible displacement. *Phys. Fluids*, 31:1330, 1988.
- [23] C. T. Tan and G. M. Homsy. Viscous fingering with permeability heterogeneity. *Phys. Fluids A*, 4:1099–1101, 1992.
- [24] A. De Wit and G. M. Homsy. Viscous fingering in periodically heterogeneous porous media. ii: Numerical simulations. *J. Chem. Phys.*, 107:9619–9628, 1997.
- [25] C. Zhang, K. Dehoff, N. Hess, M. Oostrom, T.W. Wietsma, A. J. Valocchi, B. W. Fouke, and C. J. Werth. Pore-scale study of transverse mixing induced CaCO_2 precipitation and permeability reduction in a model subsurface sedimentary system. *Environ. Sci. Technol.*, 44:7833, 2010.
- [26] C. Zhang, M. Oostrom, J. W. Grate, T. W. Wietsma, and M. G. Warner. Liquid CO_2 displacement of water in a dual-permeability pore network micromodel. *Environ. Sci. Technol.*, 45:7581, 2011.
- [27] W. B. Zimmerman and G. M. Homsy. Viscous fingering in miscible displacements : Unification of effects of viscosity contrast, anisotropic dispersion, and velocity dependence of dispersion on nonlinear finger propagation. *Phys. Fluids A*, 4:2348–2359, 1992.